SUMMARY OF THE RESISTIVE WAKE-FIELD EFFECTS IN TESLA -FEL TRANSFER LINE

M.I. Ivanian, V.M. Tsakanov

Yerevan Physics Institute,
Alikhanian Br.2, 375036 Yerevan, Armenia

Contents

1 Introduction

The specific aspect of the TESLA FEL beam is the very short bunch rms length $\sigma_z = 25\mu m$ with normalized emittance $0.7mm \cdot mrad$ that have to be transported at a distance about $12km$ to User laboratories after extraction from the main linac at energies $13 - 27GeV$ (first beamline), $23 - 50GeV$ (second beamline) [1]. The impedance of the beamline is basically dominated by the interaction of the beam with the vacuum chamber with finite conductivity producing the longitudinal and transverse wake-fields. The knowledge of the resistive wakefield effects in beamline is important for the parameter choice and cost optimization with regards to preserve the bunch energy spread and beam emittance that are required for successful SASE -FEL operation.

The behavior of the resistive wake fields have been studied by many authors[2-8]. In this report the summary of resistive wake field effects in circular metallic pipe with finite conductivity is given based on the work done by A.Chao[2] and K.Bane [3] as most exhaustive. The numerical examples of the longitudinal and transverse wake potentials induced by the TESLA-FEL beam in vacuum chamber of bending magnets and in beam pipe of a long straight section are given.

The practical MKSA units are in used. To convert the formulas in MKSA units into the equivalent form for CGS units the impedance Z_0 and permittivity ε_0 of free space have to be replaced by : $Z_0 \to 4\pi/c$, $\varepsilon_0 \to 1/4\pi$. In MKSA units $Z_0 = 377\ \Omega$, $\varepsilon_0 = 1/(36\pi 10^9)\ C/Vm$.

2 Impedance of finite conductivity pipe

Consider a point charge Q moving parallel to the z-axis at the speed of light c in an infinitely long, metallic cylindrical pipe of radius b whose axis coincides with the z-axis. Let at time $t = 0$ the charge is at location $z = 0$.The fields left by the charge are then depend on z and t only in the combination $z - ct$. The transverse position of the driving charge is $(r', \theta = 0)$ in cylindrical coordinates (r, θ). The longitudinal position variable related to the charge is then $s = ct - z$, with negative values of s located in front of the driving charge.

The conductivity of the wall material in general is dependent on the electromagnetic field frequency and is given by

$$\sigma = \frac{\sigma_0}{1 - i\omega\tau} \tag{1}$$

with the σ_0 the static conductivity, ω is a frequency of the field and τ is a relaxation time of a metal. The conductivity and relaxation time for some metals are given in Table 1. The numerical results for the induced wakefields are given for copper made vacuum chambers.

Table 1. Material properties.

Material	Static conductivity $\sigma_0(\times 10^7 \Omega^{-1} m^{-1})$	Relaxation time τ $(\times 10^{-14} s)$
Argentum	5.93	3.76
Copper	5.88	2.46
Aluminium	3.65	0.71
Stainless steel	0.14	-

The longitudinal impedance per unit length Z is given by the Fourier transform of the longitudinal electric field

$$Z(k) = -\frac{1}{Qc}\int_{-\infty}^{\infty} ds E_z(s) e^{ik_0 s}. \tag{2}$$

The result of the solution for impedance is given by A.Chao[2] as an expansion over the multipole modes

$$Z(k, r, r', \theta) = \frac{Z_0}{\pi b}\sum_{n=0}^{\infty}\frac{\cos(n\theta)}{1+\delta_{0,n}}\left(\frac{rr'}{b^2}\right)^n\left[(1+\delta_{0,n})\frac{i\lambda}{k} - \frac{ikb}{(n+1)}\right]^{-1} \tag{3}$$

where $n = 0, 1, 2$ are the monopole, dipole and quadrupole terms respectively, $\delta_{0,n}$ is the Kronecker delta function, $k = \omega/c$ and $\lambda^2 = i\sigma k Z_0$.

The longitudinal wake potential per unit length is then given by the inverse Fourier transform of the impedance

$$W_z(s) = -\frac{1}{Q}E_z(s) = \frac{c}{2\pi}\int_{-\infty}^{\infty} dk Z(k) e^{-iks} \tag{4}$$

The transverse wake potential is given by Panofsky-Wenzel theorem[9]

$$\frac{\partial}{\partial s}\mathbf{W}_\perp(\mathbf{r}, s) = -\bigtriangledown_\perp W_z(\mathbf{r}, s) \tag{5}$$

In further, the wake potentials are evaluated neglecting the very low and too high frequency contributions to impedance.

3 Longitudinal monopole wake potential

The behavior of the wake potentials are quite different at small and large distance s behind the charge and are defined by the characteristic distance s_0 that is given by pipe radius and conductivity of wall material

$$s_0 = \left(\frac{2b^2}{Z_0\sigma}\right)^{1/3} \tag{6}$$

As an example, for a copper pipe with radius $b = 1cm$, $s_0 = 20\mu m$.

3.1 Wake potential in different models.

Model 1. Static conductivity. Long wave range approach $s >> s_0$.

The longitudinal wake potential for a point driving charge is given by

$$W_z = \frac{1}{4\pi\varepsilon_0\sqrt{2\pi}b^2}\left(\frac{s_0}{s}\right)^{3/2} = \frac{1}{4\pi\varepsilon_0\sqrt{\pi Z_0\sigma}}\frac{1}{bs^{3/2}} \tag{7}$$

For the Gaussian charge distribution with rms length σ_z large compare to characteristic distance s_0 ($\sigma_z >> s_0$) the long wave range model well define the wake potential within the bunch. The monopole term for the longitudinal wake potential is given by

$$W_z(s) = -\frac{1}{8\pi\varepsilon_0 b\sigma_z^{3/2}\sqrt{2Z_0\sigma}}f(s/\sigma_z) \tag{8}$$

with

$$f(u) = |u|^{\frac{3}{2}}\, e^{-\frac{u^2}{4}}\left(I_{1/4} - I_{-3/4} \mp I_{-1/4} \pm I_{3/4}\right)\,|_{u^2/4} \tag{9}$$

where I is a modified Bessel function; the upper signs apply for $u < 0$, the lower signs for $u > 0$.

The RMS energy spread $\sigma_\in$ and the longitudinal loss factor k_z are then given by

$$\sigma_\in = eQ\left[\int_{-\infty}^{\infty} ds\rho(s)W_z^2(s) - k_z^2\right]^{1/2} = \frac{0.46eQ}{2\pi^2\varepsilon_0 b\sigma_z^{3/2}\sqrt{Z_0\sigma}} \tag{10}$$

$$k_z = \int_{-\infty}^{\infty}\rho(s)W_z(s)ds = \frac{\Gamma\,(3/4)}{2\pi^2\varepsilon_0 b\sigma_z^{3/2}\sqrt{2Z_0\sigma}} \tag{11}$$

The maximum and minimum absolute value of $f(u)$ within the bunch is equal $f_{\min} = f(-0.56) = -1.705$; $f_{\max} \approx f(1.74) \approx 0.7835$ and the peak-to-peak energy spread ΔE is then given by

$$\Delta E = eQ\,|W_{z\,\max} - W_{z\,\min}| = \frac{2.4885}{8\pi\varepsilon_0 b\sigma_z^{3/2}\sqrt{2Z_0\sigma}} \tag{12}$$

Putting in constants we get

$$k_z = 2.522\left[\frac{V\cdot m}{nC\cdot\Omega^{1/2}}\right]\frac{1}{b\sigma_z^{3/2}\sigma^{1/2}} \tag{13}$$

$$\sigma_\in = 0.136\left[\frac{V\cdot m}{nC\cdot\Omega^{1/2}}\right]\frac{eQ}{b\sigma_z^{3/2}\sigma^{1/2}} \tag{14}$$

$$\Delta E = 0.408\left[\frac{V\cdot m}{nC\cdot\Omega^{1/2}}\right]\frac{eQ}{b\sigma_z^{3/2}\sigma^{1/2}} \tag{15}$$

The numerical simulation study including short range wakes shows that the formulas based on long wake approximation are valid for the bunch rms length $\sigma_z \geq 4s_0$.

As an example is the resistive wake that will be induced by TESLA beam $\sigma_z = 0.3mm$ in copper vacuum chamber of a bending magnets at the part of the transition at 55 GeV. For copper vacuum chamber the results are valid for chamber radius $r \leq 10cm$ ($s_0 \leq 0.1mm$) . For pipe radius $b = 3cm$, the characteristic distance $s_0 = 40\mu m$,and the rms and peak-to-peak induced correlated energy spread per unit length are $\sigma_\epsilon = 0.24KeV/m$, $\Delta E = 0.75KeV/m$. For 40m length of the magnet these correspond to 9.6 and 30 KeV energy spread.

Model 2. Static conductivity. Short and long range wakes.

Short range longitudinal monopole wake potential for static conductivity including the low and high frequency part of the impedance is given by

$$w_z(s) = -\frac{4}{\pi\varepsilon_0 b^2}\left(\frac{1}{3}e^{-s/s_0}\cos\frac{\sqrt{3}s}{s_0} - \frac{\sqrt{2}}{\pi}\int_0^\infty dx\frac{x^2e^{-x^2s/s_0}}{x^6+8}\right) \tag{16}$$

Model 3. Frequency dependent conductivity. Short and long range wakes.

The impedance is then given by

$$Z(k) = \frac{Z_0 s_0}{2\pi b^2}\left[\sqrt{\frac{t_\lambda}{\Gamma k^2}}\left(i\sqrt{1+t_\lambda} + sgn(k)\sqrt{1-t_\lambda}\right) - \frac{ik}{2}\right]^{-1} \tag{17}$$

where $k_0 = s_0 k$ is a dimensionless wavenumber, $\Gamma = \tau c/s_0$ is a dimensionless metal relaxation time and $t_\lambda = |k_0|\,\Gamma/\sqrt{1+k_0^2\Gamma^2}$. The wake potentials for high Γ limit may be presented as follows:

$$w_z = -\frac{1}{\pi\varepsilon_0 b^2}e^{-s/4\Gamma s_0}\cos\left[\left(\frac{8}{\Gamma}\right)^{1/4}\frac{s}{s_0}\right] \tag{18}$$

For arbitrary Γ the wake potential is calculated numerically.

Model 4. Ultra-short range approach .

In an ultrashort case, when the bunch rms length σ_z is small compare to characteristic distance s_0 the wake potential is mainly influenced by the wake at ultrashort distances, with an approximately constant amplitude given by

$$w_z(s) = -\frac{1}{\pi\varepsilon_0 b^2} \tag{19}$$

which is independent of the conductivity of the wall material. The wake potential within the Gaussian bunch is then given by error-function

$$W_z(s) \simeq -\frac{1}{\pi\varepsilon_0 b^2}\int_{-\infty}^{s}\rho(s')ds' = -\frac{1}{2\pi\varepsilon_0 b^2}\left[1+\mathrm{erf}\left(\frac{s}{\sqrt{2}\sigma_z}\right)\right] \tag{20}$$

with the loss factor and rms energy spread given by

$$k_z = \frac{1}{2\pi\varepsilon_0 b^2} = 18\left[\frac{V\cdot m}{nC}\right]\frac{1}{b^2} \tag{21}$$

$$\sigma_\in = 0.289\frac{eQ}{\pi\varepsilon_0 b^2} = 10.4\left[\frac{V\cdot m}{nC}\right]\frac{eQ}{b^2} \tag{22}$$

$$\Delta E \simeq |W_z(3\sigma_z) - W_z(-3\sigma_z)| \simeq \frac{eQ}{\pi\varepsilon_0 b^2} = 36\left[\frac{V\cdot m}{nC}\right]\frac{eQ}{b^2} \tag{23}$$

As an example for the copper pipe radius of $b = 15cm$ the characteristic distance $s_0 = 120\mu m$ ($\sigma_z/s_0 \sim 0.2$). The induced RMS and peak-to-peak energy spread at 10 km are: $\sigma_\in = 4.6MeV$ and $\Delta E = 16MeV$.

3.2 Longitudinal monopole wake for FEL beam.

Fig.1 shows the longitudinal wake potentials for TESLA FEL gaussian bunch ($\sigma_z = 25\mu m$) for two values of the pipe radius $b = 5cm, 10cm$ using the model of static(solid line) and frequency dependent (dashed line) conductivity and including the short and long range contribution to the wake potential. For comparison the wake potential in long range approach for $b = 5cm$ case is given by dotted line.

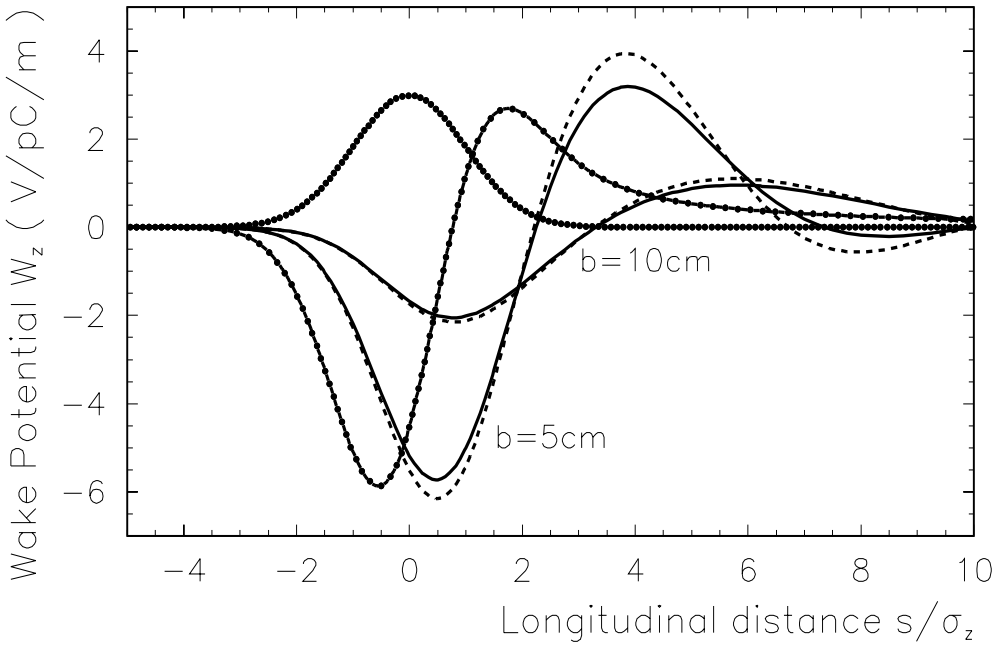

Fig.1 *Longitudinal wake potentials for TESLA-FEL gaussian bunch ($\sigma_z = 25\mu m$) for pipe radius $b = 5cm$ and $b = 10cm$. The solid and dashed curves correspond to the models of static and frequency-dependent conductivity. For comparison, the long range approach (dotted curve) for $b = 5cm$ is shown. Material - copper.*

Fig.2 shows the rms (a), peak-to-peak (b) and maximal (c) energy spread versus of the beam pipe radius for the TESLA FEL beam. The solid line -static conductivity, the dashed line - frequency dependent conductivity. For comparison shown the long ($\sigma_z \gg s_0$) and ultra-short ($\sigma_z \ll s_0$) bunch approaches.

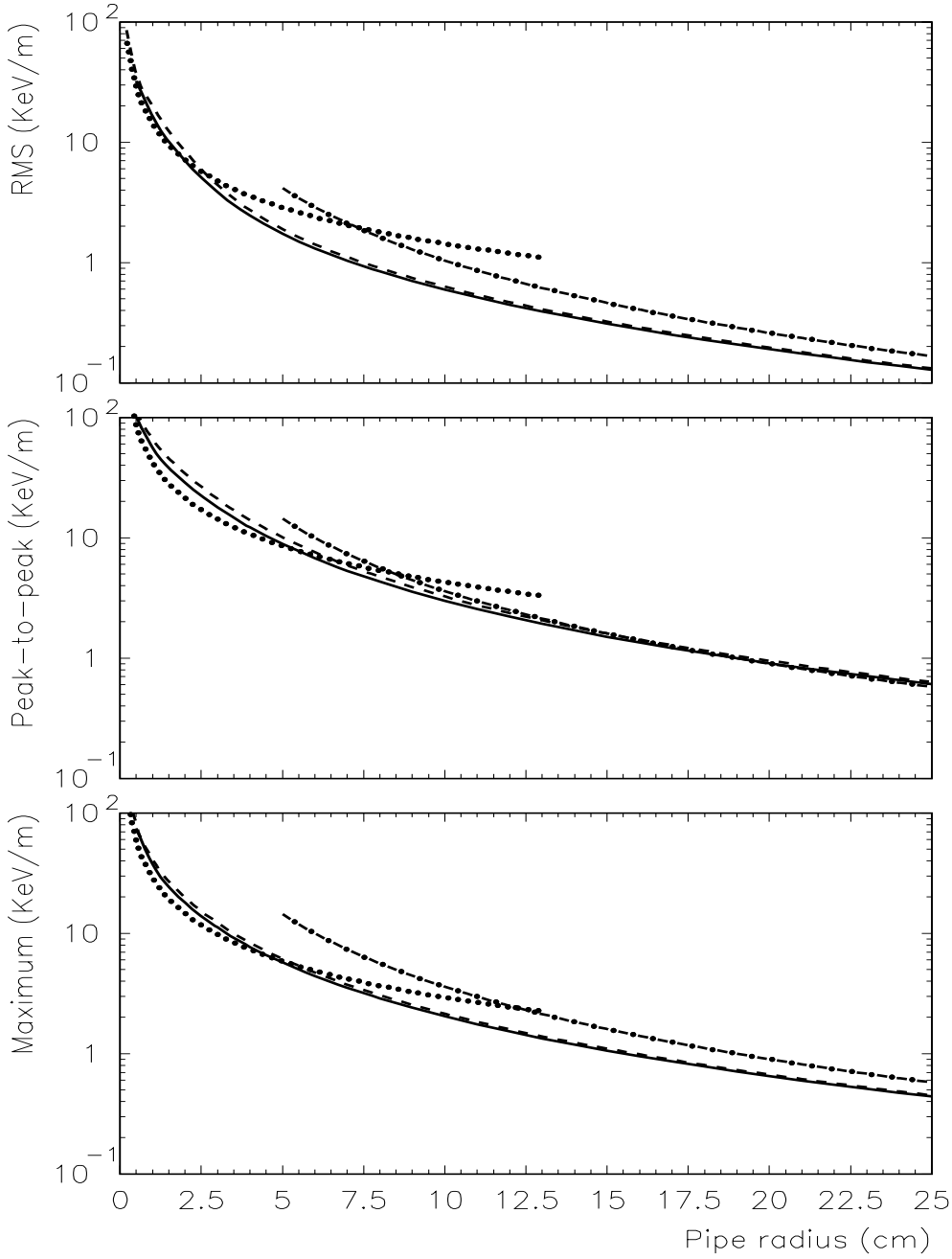

Fig.2 *RMS (a), peak-to-peak (b) and maximal (c) energy spread versus of the beam pipe radius calculated by the static (solid curve) and frequency-dependent (dashed curve) conductivity models. Also shown the long range (dotted curve) and ultra-short (marked curve) approaches. Material - copper.*

Fig.3 shows the longitudinal wake potential of TESLA FEL beam for the pipe radius $b = 15cm$ with static (solid line) and frequency dependent (dashed line) conductivity. The RMS and peak-to-peak energy spread for pipe length 12 Km are equal 3.8 and 13.2 MeV respectively.

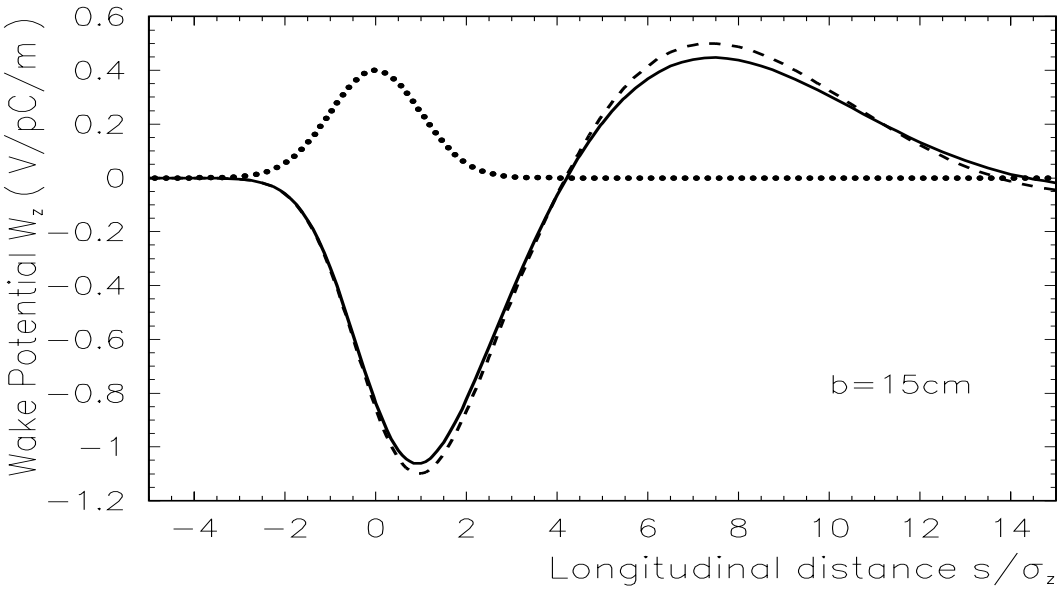

Fig.3. *Longitudinal wake potentials for TESLA-FEL gaussian bunch ($\sigma_z = 25\mu m$) for pipe radius ($b = 15cm$), calculated using static (solid curve) and frequency-dependent (dashed curve) conductivity models. Material-copper.*

3.3 Induced energy spread in TESLA- FEL transfer line.

The tolerable RMS correlated energy spread of the beam for successful operation of the SASE-FEL is estimated at the level of 10^{-3}. For minimum operation energy of the SASE-FEL at 13 GeV, these correspond to induced energy at the level of 13 MeV.

Two main parts of the FEL beamline that are the substantial source of the resistive wakes are :

1) the elliptical vacuum chamber of the bending magnets with the total length of about 500m and small vertical half-aperture (b$\sim$1.5cm);

2) the round vacuum chamber for beam transport to 12 km after extraction from the main linac (two beamlines in energy range 13-27 GeV and 23-50GeV).

Induced energy spread in bending magnets.

As it follow from the Fig.1 for longitudinal wake potentials of FEL beam, for pipe radius below 5cm, the maximum energy deviation within the range $(-3\sigma_z, 3\sigma_z)$ is defined by peak-to-peak energy deviation (Fig.2) and the induced absolute value of energy deviation per unit length induced in pipe of radius

b=1.5cm is 46 KeV/m. For 500m of the vacuum chamber the energy deviation is then 23 MeV.

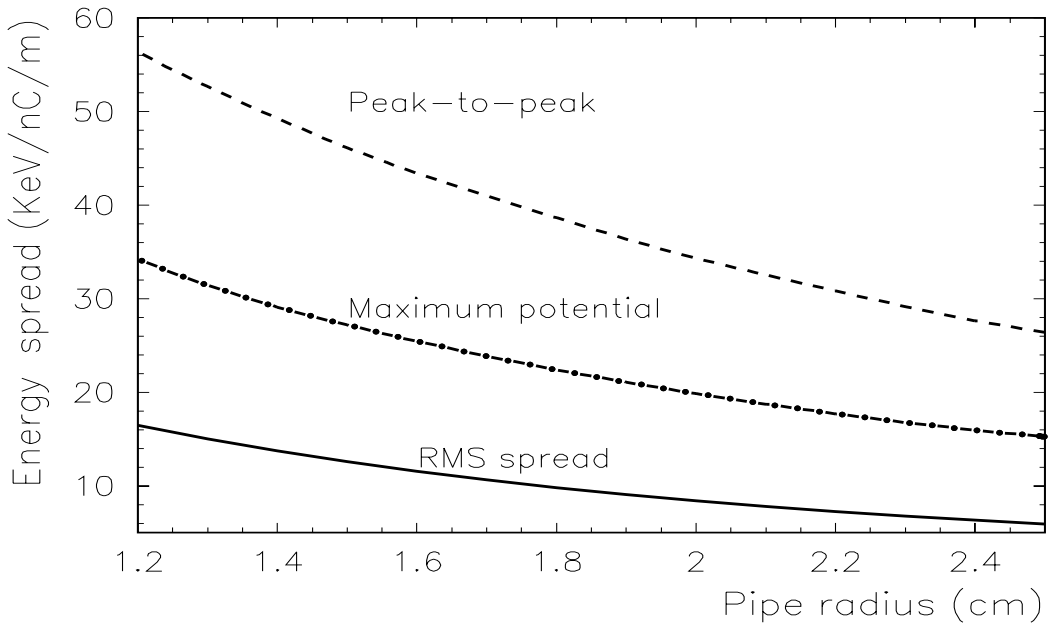

Fig.4 *Energy spread in small resistive pipe with the frequency dependent conductivity. Material-copper.*

Table 2. Energy spread in small pipe.

Vertical half aperture $b\ (mm)$	10	12	15	20	25
Peak-to-peak energy deviation $\Delta E_p(\ KeV/nC/m)$	66	56	46	34	26
Maximum retarding potential $\Delta E_m(KeV/nC/m)$	41	34	27	20	15
Total peak-to-peak deviation $\Delta E_{p\ total}(MeV)$	33	28	23	17	13
Total max retarding induced energy $\Delta E_{m\ total}(MeV)$	21	17	14	10	7.6
RMS energy spread at 500 m $\sigma_\epsilon(MeV)$	10	8.2	6.3	4.2	3.0

Taking into account that the long wave model for a round pipe and two parallel infinite plates gives the same monopole longitudinal wake potential [2,6] when the bunch width small compare to geometrical size of vacuum chamber, the above numbers well estimate the resistive wake effect in elliptical vacuum chamber of a bending magnets. Table 2 presents the induced energy spread for different aperture of the vacuum chamber.

Induced energy spread in straight beamline.

As it follow from the Fig.1 for longitudinal wake potentials of FEL beam, for pipe radius above 10 cm, the peak-to-peak energy deviation within the range $(\ -3\sigma_z, 3\sigma_z)$ is defined by maximum retarding potential (Fig.2). The induced peak-to-peak energy deviation per unit length induced in pipe of radius b=15cm

is 1.1 KeV/m. For 12km of the vacuum chamber the total peak-to-peak energy deviation is then 13.2 MeV.

Table 3. Energy spread in large pipe.

Radius of the pipe b (mm)	100	120	150	175	200
Max retarding potential $\Delta E_m(\ KeV/nC/m)$	2.15	1.6	1.1	0.84	0.67
Total energy deviation at 12km (MeV)	25.8	19.1	13.2	10.1	8.04
RMS energy spread at 12km $\sigma_\epsilon(MeV)$	7.55	5.6	3.87	2.97	2.36

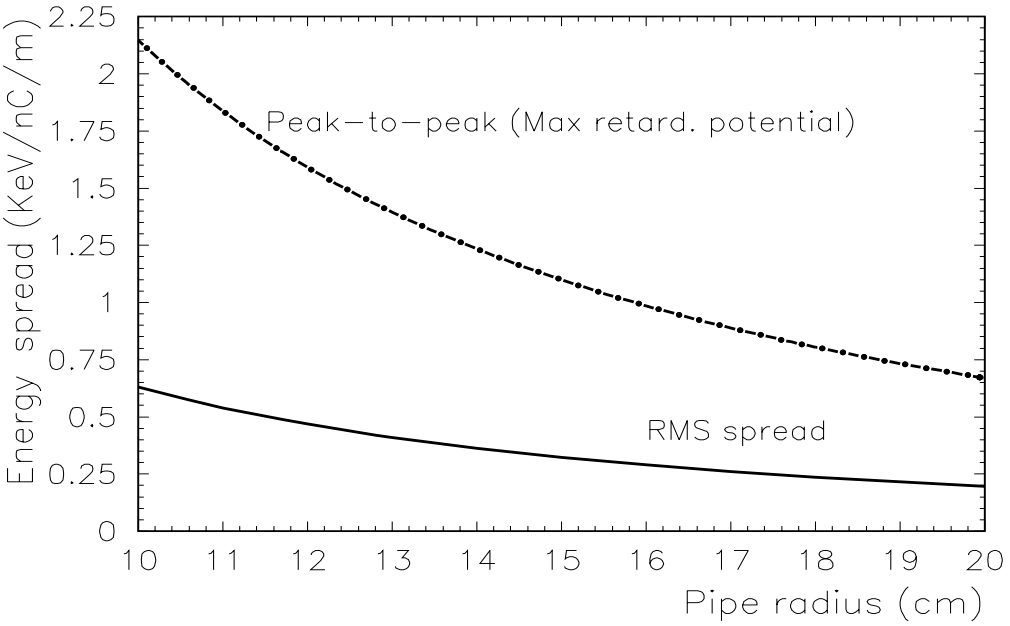

Fig.5. *Energy spread in large resistive pipe with the frequency dependent conductivity. Material-copper.*

Resulting energy spread

The total induced energy in the beam is the superposition of the induced energy in bending magnet elliptical vacuum chamber and in round pipe of straight beamline.

$$\Delta E(s) = eQ\left[L_b W_z^b(s) + L_B W_z^B(s)\right] \tag{24}$$

where L_b, L_B are the length of the small and large vacuum pipes. The two sources (small and large pipes) of resistive wakes produce the different type of wakes: while the wake in small pipe is close to long range approach, the wake in large pipe is close to short range approach. And as clear follow from the shape of the wake potentials (Fig.1), the peak-to peak total energy spread is defined by the maximum retarding wake potentials when the maximum induced potentials in two parts of transfer line are at the same order. As an example, Fig.6 presents

the total induced energy deviation within the bunch after FEL beam passes 500 m pipe of radius 15mm and 12 km pipe of radius 15cm.

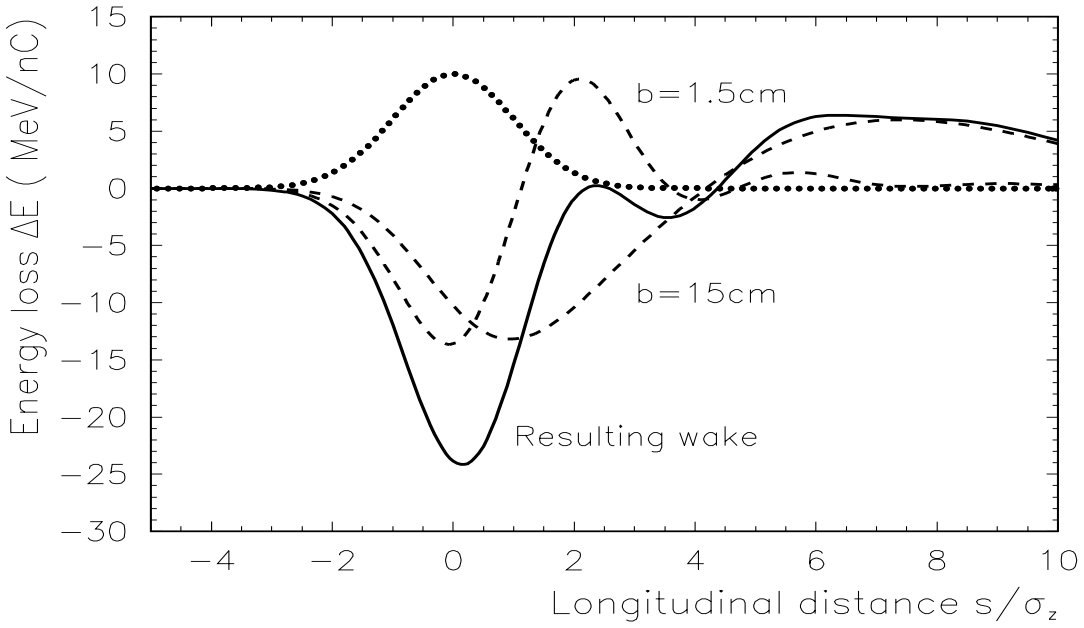

Fig.6 *Resulting induced energy spread in FEL bunch (solid line) after passing the 500 m long vacuum chamber of bending magnets (b=1.5cm) and 12 km long transfer line (b=15cm). Dashed lines show the induced energy in each part of transfer line. Material -copper.*

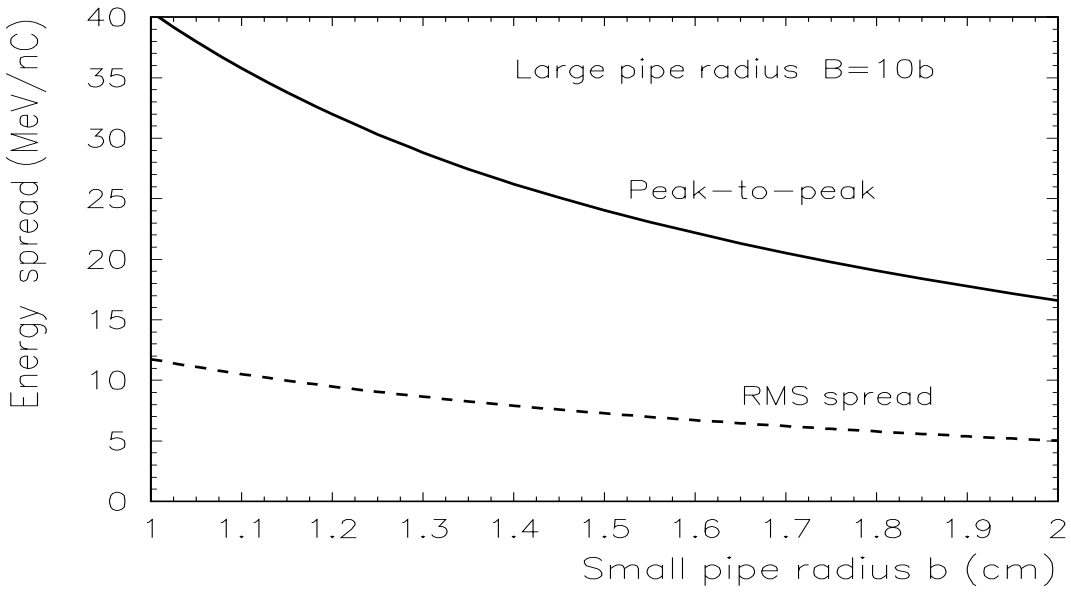

Fig.7 *Induced resulting energy spread versus of beam pipe radius. The length of the large and small pipes are* $L_b = 500m, L_B = 12km$ *respectively. The pipe radii are related as B=10b. Material-copper.*

Fig.7 shows the resulting RMS and peak-to peak energy spread for the FEL beam in whole transfer line. The radii of the small (b) and large (B) pipes in two parts of the transfer line are related as $B = 10b$.

The numerical values for energy spread is presented in Table 4.

Table 4. The resulting energy spread.

Radius of the pipes $b\ (cm)/B(cm)$ $L_b = 500m, L_B = 12km$	1./10	1.2/12	1.5/15	1.75/17.5	2.0/20
Average energy loss $\Delta E_{av}(MeV)$	27.5	22	16.3	13.5	11.2
Peak-to -peak energy spread (MeV)	40	32	24	19.7	16.5
RMS energy spread $\sigma_{\in}(MeV)$	11.8	9.5	7.2	6.0	5.0

4 Transverse dipole wake potential

4.1 Dipole wake in different model

Model 1. Static conductivity, long wave range approach ($s >> s_0$).

The transverse wake potential for a point charge is given by

$$w_{\perp}(s) = \frac{1}{\pi^{3/2}\varepsilon_0\sqrt{Z_0\sigma}} \cdot \frac{r}{b^3} \cdot \frac{1}{s^{1/2}} \tag{25}$$

For gaussian bunch the dipole wake read as

$$W_{\perp}(s) = \frac{r}{2\pi\varepsilon_0 b^3 \sigma_z^{1/2}\sqrt{2Z_0\sigma}} f_{\perp}(s/\sigma_z) \tag{26}$$

with

$$f_{\perp}(u) = |u|^{1/2}\, e^{-u^2/4} \left(I_{-1/4} \pm I_{1/4}\right) |_{u^2/4} \tag{27}$$

The maximum of the transverse wake potential is reached at s$\approx \sigma_z$ and is given by

$$W_{\perp \max} = \frac{1.67x}{2\pi\varepsilon_0 b^3 \sigma_z^{1/2}\sqrt{2Z_0\sigma}} = 1.095 \left[\frac{V \cdot m}{nC \cdot \Omega^{1/2}}\right] \frac{r}{b^3 \sigma_z^{1/2}\sigma^{1/2}} \tag{28}$$

and the transverse loss factor is given by

$$k_r = \frac{\Gamma(1/4)}{2\pi^2\varepsilon_0\sqrt{2Z_0\sigma}} \frac{r}{b^3\sigma_z^{1/2}} = 0.756 \left[\frac{V \cdot m}{nC \cdot \Omega^{1/2}}\right] \frac{r}{b^3 \sigma_z^{1/2}\sigma^{1/2}} \tag{29}$$

For two-particle model of the bunch , the special interest is the transverse wake potential of a point charge at the distance $s = 2\sigma_z$

$$w_{\perp}(2\sigma_z) = \frac{1}{\pi^{3/2}\varepsilon_0\sqrt{2Z_0\sigma}} \cdot \frac{r}{b^3\sigma_z^{1/2}} = 0.74 \left[\frac{V \cdot m}{nC \cdot \Omega^{1/2}}\right] \frac{r}{b^3 \sigma_z^{1/2}\sigma^{1/2}} \tag{30}$$

Model 2. Static conductivity. Short and long range wakes.

Short range dipole wake potential [3]

$$W_\perp(s) = \frac{2r}{3\pi\varepsilon_0 b^4} s_0 \left\{ e^{-s/s_0} \left[\sqrt{3} \sin\left(\sqrt{3}s/s_0\right) - \cos\left(\sqrt{3}s/s_0\right) \right] + \frac{12\sqrt{2}}{\pi} \int_0^\infty dx \frac{e^{-x^2 s/s_0}}{x^6+8} \right\} \tag{31}$$

Model 3. Frequency dependent conductivity. Short and long range wakes.

The potential is calculated numerically.

Model 4. Ultra-short range approach

In an ultrashort case, when the bunch rms length σ_z is small compare to characteristic distance s_0 the wake potential is mainly influenced by the wake at ultrashort distances, with an approximately constant amplitude given by

$$w_\perp(s) = \frac{2r}{\pi\varepsilon_0 b^4} s \tag{32}$$

which is independent of conductivity of the wall material. The transverse wake potential within the Gaussian bunch is given by error-function

$$W_\perp(s) \simeq \frac{2r}{\pi\varepsilon_0 b^4} \int_{-\infty}^{s} \rho(s')(s-s')ds' = \frac{r}{\pi\varepsilon_0 b^4} \left[s + s \cdot \mathrm{erf}\left(s/\sqrt{2}\sigma_z\right) + \sqrt{\frac{2}{\pi}}\sigma_z e^{-s^2/2\sigma_z^2} \right] \tag{33}$$

with the transverse loss factor

$$k_z = \int_{-\infty}^{\infty} W_\perp(s')\rho(s')ds' = \frac{2\sigma_z r}{\pi^{3/2}\varepsilon_0 b^4} = 40.6 \left[\frac{V\cdot m}{nC}\right] \frac{\sigma_z r}{b^4} \tag{34}$$

and the transverse wake potential of point charge at the distance $s = 2\sigma_z$

$$w_\perp(2\sigma_z) = \frac{4r\sigma_z}{\pi\varepsilon_0 b^4} = 144 \left[\frac{V\cdot m}{nC}\right] \frac{\sigma_z r}{b^4} \tag{35}$$

4.2 Transverse dipole wake for TESLA-FEL beam

Fig.8 shows the transverse wake potentials for TESLA FEL gaussian bunch ($\sigma_z = 25\mu m$) for two values of the pipe radius $b = 5cm, 10cm$ using the model of static(solid line) and frequency dependent (dashed line) conductivity and including the short and long range contribution to the wake potential. For comparison the wake potential in long range approach is given by dotted line.

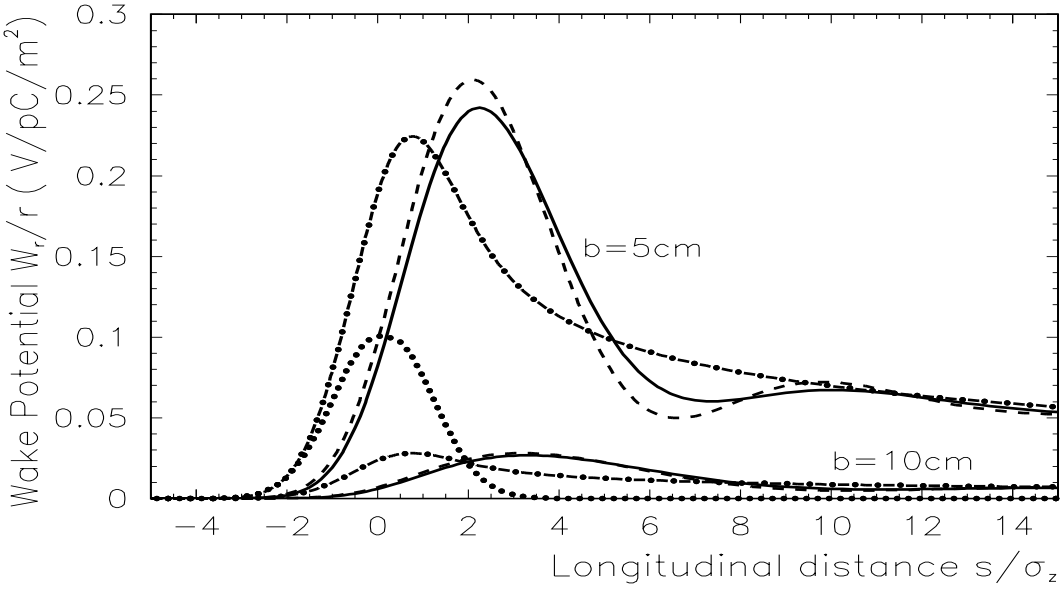

Fig.8 *Transverse wake potentials for TESLA-FEL gaussian bunch ($\sigma_z = 25\mu m$) for pipe radius $b = 5cm$ (1) and $b = 10cm$ (2). The solid,dashed and dotted curves correspond to the models of static conductivity, frequency-dependent conductivity and long range approach respectively.*

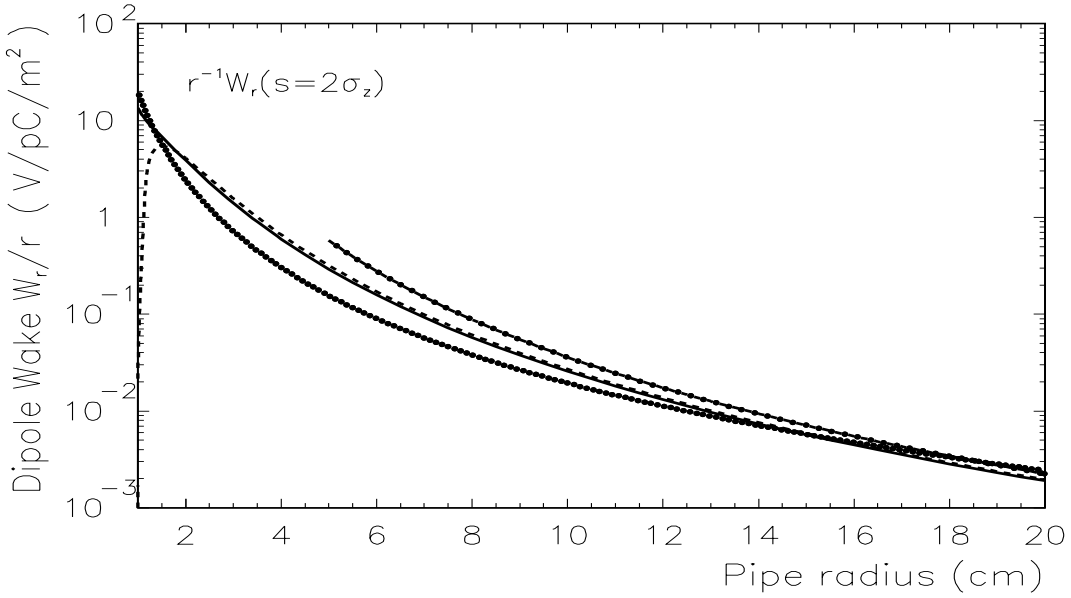

Fig.9 *Transverse wake potential for the point-like charge at the distance $s = 2\sigma_z$ versus of the pipe radius for static (solid curve), frequency-dependent (dotted line), long -range (dashed line) and ultra-short (dot-dashed line) models.*

Fig.9 shows the transverse wake potential at the distance s=$2\sigma_z$ versus of the pipe radius for static and frequency dependent conductivity. The transverse wake potential for the pipe radius $b = 15cm$ is shown in Fig.10.

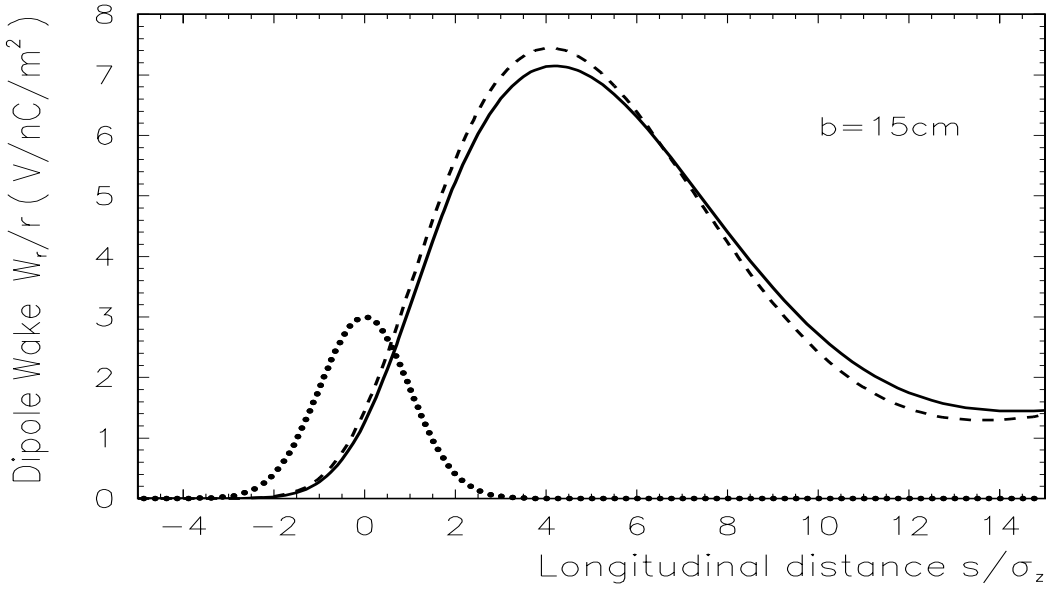

Fig.10 *Transverse wake potentials for TESLA-FEL gaussian bunch ($\sigma_z = 25\mu m$) for pipe radius $b = 15cm$. Shown the results for static (solid line) and frequency-dependent (dashed line) conductivity models. Material -copper.*

4.3 Transverse wake field effects.

The first beamline should be suitable for whole energy range 13-27 GeV. The optical solution for periodic FODO lattice is given by relation

$$sin\frac{\mu_1}{2} = \frac{E_2}{E_1} sin\frac{\mu_2}{2} \tag{36}$$

with E_2, μ_2 the energy and phase advance per cell for high energy beam (27 GeV), E_1, μ_1 the energy and phase advance per cell for low energy beam (13 GeV). The reasonable values for phase advance per cell are then $\mu_1 = 100$ and $\mu_2 = 45$ degrees.

Emittance enlargement by transverse wakefield.

Consider the free coherent oscillation of the FEL beam in 12 km long beamline that is contain of periodic FODO lattices. The beam is enter to beamline with one standard initial offset. A good analytical prediction of the emittance enlargement by transverse wakefields is follow from the two-particle model of the bunch. The beam is modeled by two macro-particles with the charge $Q/2$ that are separated by the longitudinal distance $\Delta s = 2\sigma_z$, where σ_z is the rms length of the bunch. The first, heading particle feels no transverse wakefield and thus undergoes free betatron oscillations with initial amplitudes x_0, x_0'. The second , trailing particle experiences the dipole wake potential $w_d = w_x(2\sigma_z)$ due to off-axis motion of the

leading particle. With neglect of dispersive effect, the emittance enlargement for one sigma offset is then given by

$$\frac{\Delta\varepsilon}{\varepsilon_0} = \frac{1}{2}\left(\frac{eQw_d}{8E_0}\right)^2 \frac{1}{sin^2\mu}\frac{L^4}{N_{cell}^2} \tag{37}$$

with ε_0 natural beam emittance, E_0 - design particle energy, μ -the phase advance per FODO cell , L -the total length of beamline and N number of FODO cells.

Emittance dilution by longitudinal wakefield.

The emittance dilution is dispersive. The relative correlated rms energy spread along the beamline increase as

$$\delta_{rms}(z) = \frac{\sigma_\in}{E_0} z \tag{38}$$

with $\sigma_\in$ induced rms energy spread per unit length in resistive pipe. The emittance dilution for one standard offset is then given by

$$\frac{\Delta\varepsilon}{\varepsilon_0} \approx \frac{a_0^2}{\varepsilon_0}\left(\frac{\sigma_\in L}{E_0}\right)^2 (N_{cell}-1)^2 \cdot tan^2\frac{\mu}{2} \tag{39}$$

Uncorrelated dispersive emittance dilution.

For the initial rms uncorrelated energy spread δ_{un} , the emittance dilution is

$$\frac{\Delta\varepsilon}{\varepsilon_0} = 2\frac{a_0^2}{\varepsilon_0}\delta_{un}^2 N_{cell}^2 \cdot tan^2\frac{\mu}{2} \tag{40}$$

The optical parameters and expected emittance enlargement for one sigma offset ($a_0^2 = \varepsilon$) and pipe radius 15 cm is presented in Table 5. The phase advance per cell for low energy (E=13GeV) and high energy (E=27 GeV) beams are $\mu_1 = 100$ degree and $\mu_2 = 45$ degree respectively.

Table 5. Emittance dilution for $E = 13GeV$ FEL beam.

Number of FODO cell	20	30	40	50
Cell length	600	400	300	240
Max β value E=27 GeV (m)	1170	780	585	468
Max β value E=13 GeV (m)	1074	716	537	430
Emitt. dilution by trans. wake	$1.2{\cdot}10^{-7}$	$0.55{\cdot}10^{-7}$	$0.3{\cdot}10^{-7}$	$0.18{\cdot}10^{-7}$
Emitt. dilution by long. wake	$6.2{\cdot}10^{-5}$	$1.55{\cdot}10^{-4}$	$2.5{\cdot}10^{-4}$	$4.2{\cdot}10^{-4}$
Uncorrelated dispersive dilut.	$1.1{\cdot}10^{-3}$	$2.5{\cdot}10^{-3}$	$4.5{\cdot}10^{-3}$	$7.1{\cdot}10^{-3}$
$w_x(2\sigma_z) = 6.1V/nC/m^2$, $\sigma_\in = 0.2KeV/m$, $\delta_{un} = 10^{-3}$, $\mu_1 = 100\ deg.$				

Thus, the emittance dilution in 12 km straight line with pipe radius at the level of $b = 15cm$ is dominated by dispersive effects. If the suitable matching optics is available then the number of the FODO cell is reasonable to keep as small as possible.

Transfer line of bending magnets.

Consider the vertical emittance dilution due to transverse resistive dipole wake induced in small vacuum chamber (b=1.5cm) of bending magnets with the total length of 500m. The beam is enter to magnet with one standard offset. Assuming the smooth variation of betatron function in bending magnets, the emittance dilution of the beam is given by

$$\frac{\Delta\varepsilon}{\varepsilon_0} = \frac{1}{2}\frac{a_0^2}{\varepsilon_0}\left(\frac{eQw_d}{8E_0}\right)^2 L_b^4 \tag{41}$$

where L_b is the total length of the bending magnet. The dipole wake per unit length at a distance of s=$2\sigma_z$ induced by a point charge in a copper vacuum chamber with radius b=1.5cm is equal to $w_x(2\sigma_z) = 8KeV/nC/m^2$. The expected maximum emittance dilution at the distance $L_b = 500m$ is then $\Delta\varepsilon/\varepsilon_0 = 2.6\cdot10^{-4}$.

5 Aluminium and stainless steel type materials.

In this section we give the induced energy spread in FEL beam for a pipes with aluminium and stainless type materials. Tables 6 and 7 present the induced energy spread in transfer line that includes the resistive longitudinal wakes in the vacuum chamber of bending magnets (vertical aperture b=1.2cm, 500 m long) and in round pipe of long beamline (radius B=12cm, 12 km long).

Table 6. RMS energy spread for different metals (MeV).
B=12cm, b=1.2cm.

	Copper	Aluminium	Stainless
Small pipe	8.2	8.55	18.5
Large pipe	5.6	5.9	7.6
Total	9.5	10.56	25.6

Table 7. Peak - to -peak energy spread for different metals (MeV).
B=12cm, b=1.2cm.

	Copper	Aluminium	Stainless
Small pipe	28.2	31.8	63.2
Large pipe	19.1	20.2	27.6
Total	32	36.3	90.35

The rms, maximum retarding potential and peak-to-peak energy spread induced by FEL beam in large and small pipes made from aluminium and stainless steel type materials are shown in Fig.11-14.

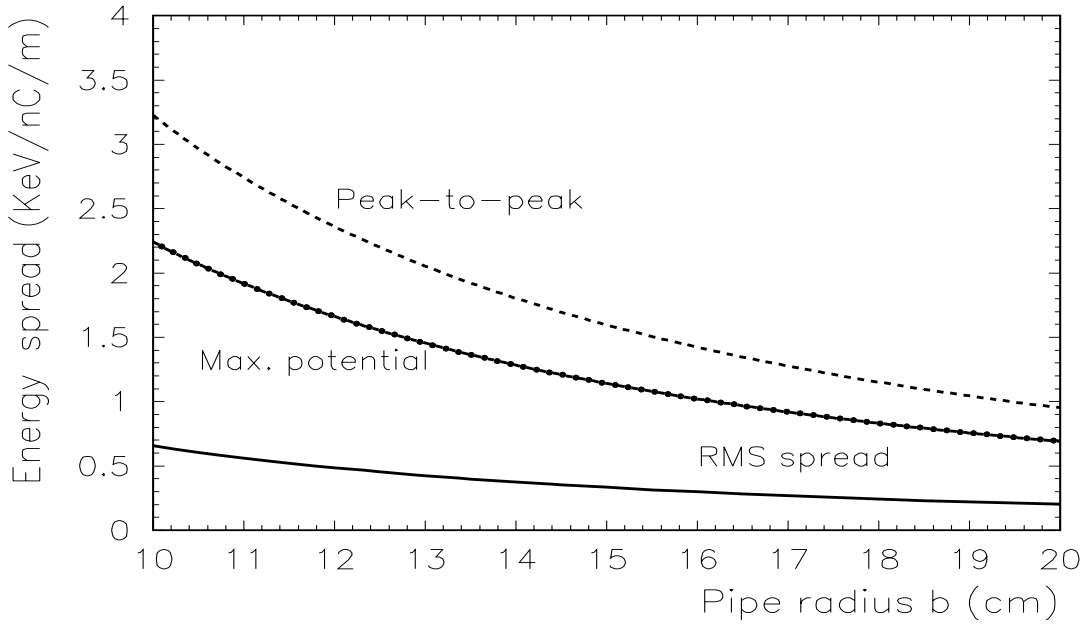

Fig.11. *Induced energy spread in aluminium large pipe.*

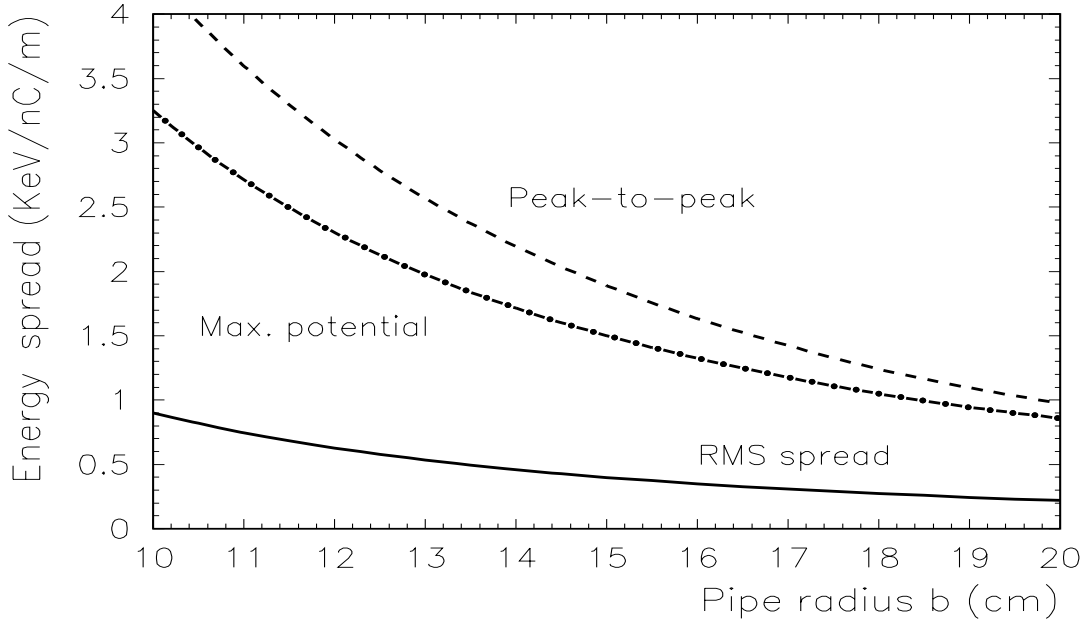

Fig.12. Induced energy spread in stainless large pipe.

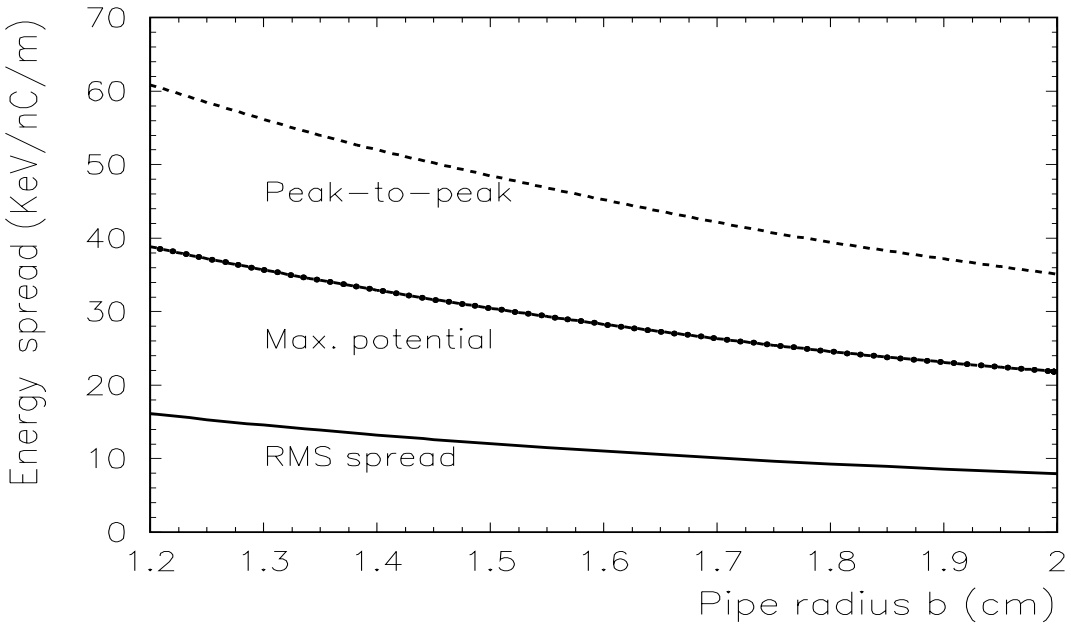

Fig.13 Induced energy spread in aluminium small pipe.

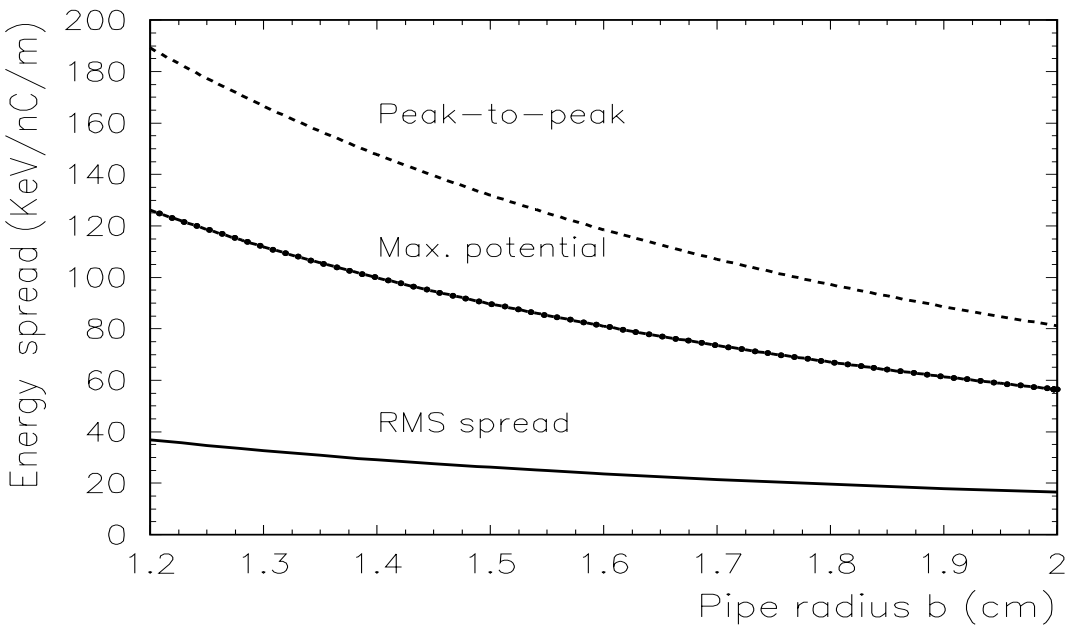

Fig.14. Induced energy spread in stainless small pipe.

6 Summary

Based on the study of the resistive wakefield effects in vacuum pipe of the transfer line, the following conclusions can be made.

- The suitable material for beam pipe is aluminium both from the induced energy and cost optimization point of view.
- The reasonable value of pipe radius in long 12 km straight line is b=12cm.
- The vertical half-aperture in bending magnets 1.4-1.6cm.
- The total peak- to-peak induced energy spread is then at the level of $\Delta E = 32MeV$
- The RMS energy spread is at the level of $\sigma_{rms} = 10MeV$
- The emittance dilution in straight line is dominated by dispersive effect and for one sigma coherent oscillations is at the level of 10^{-4}.
- The reasonable number of quadrupoles in 12 km long transfer line is 60-80 (30-40 FODO cells).
- The maximum emittance enlargement in bending magnets is at the level of $4{\cdot}10^{-4}$ for one sigma offset of the beam.

Acknowledgement

Authors thank Martin Dohlus and Klaus Floettmann for very helpful disscussions. Special thanks to Reinhard Brinkmann and Joerg Rossbach for their interest and support of this work.

Reference

1. Conceptual Design of a 500 GeV e^+e^- Linear Collider with Integrated X-ray Laser Facility. Edited by R. Brinkmann, G.Materlik, J.Rosbach, A.Wagner, DESY 1997-048, 1997.

2. A. Chao. Coherent Instabilies of a Relativistic Bunched Beam. Technical Report 2946, SLAC-PUB, 1982.

3. K.Bane. SLAC-AP-87 (May 1991).

4. O. Henry and O. Napoly. The resistive pipe wake potentials for short bunches. Part. Accel. 35, 235-248 (1991) and CERN-CEA, DPhN/STAS/01-R08 (May 1991).

5. K.L.F. Bane and M. Sands. The short-range resistive wall wakefields. SLAC-PUB-95-7074, 19p. (1995).

6. H.Henke, O.Napoly. in *Proc. of the 2nd European Particle Accelerator Conference,*Nice, France, Edition Frontiers,1990, p.1046.

7. A. Piwinski. Wake fields and ohmic losses in round vacuum chambers. Technical Report DESY HERA 92-11, Deutsches Electronen Synchrotron, DESY, May 1992.

8. H. Schlarb. Resistive wall wake fields. Diplomarbeit zur Erlangung des Grades eines Diplomphysikers. Hamburg, August 1997.

9. W. Panowsky, W. Wenzel. *Rev. Sci. Instrum.* **27**, 967 (1956).